COMPARATIVE STUDY OF THE VISCOELASTICITY OF PARYLENE THIN FILMS FOR MEMS USING NANO-DMA AND MOLECULAR DYNAMICS

Wenshu Sui[1], Maxime S. Duvieusart[1], Junhua Zhao[2], Yu-Chong Tai[3] and Yi-Kuen Lee[1]
[1]The Hong Kong University of Science and Technology, HONG KONG SAR
[2]Jiangnan University, Wuxi, CHINA
[3]California Institute of Technology, Pasadena, CA 91125, USA

ABSTRACT

We present a comparative study of the viscoelasticity of parylene C (PPXC) by using Nano-DMA (Dynamical Mechanical Analysis) and Molecular Dynamics (MD) simulations. By applying sinusoidal loading on PPXC films at different temperatures and frequencies, the complex modulus and glass transition temperature (T_g) of the PPXC were obtained. The predicted T_g determined from the temperature-dependent density change in the MD model is consistent with the results in our measurements and previous works. Furthermore, with Time-Temperature Superposition Principle (TTSP), we successfully determined the master curve of PPXC, for the first time, which is critical for the parylene reliability study of bio-MEMS devices.

INTRODUCTION

Parylene has been widely used in MEMS technology because of its excellent material properties (conformal deposition, biocompatibility, etc.). However, many researchers mainly focus on studying parylene's elastic properties (such as Young's modulus), but not on the viscoelasticity [1-2]. It is well known that viscoelastic behaviors of polymers significantly differ below and beyond glass transition temperature (T_g). Moreover, though some research papers reported the T_g values of parylene C (PPXC) measured by different methods, there is a lack of consistent reported T_g of PPXC, ranging from 35 to 150°C [3-5].

One of the most commonly used ways to characterize T_g is the Differential Scanning Calorimetry (DSC) test. The basic principle underlying this technique is that when the sample undergoes a physical transformation, such as phase transitions, a sudden increase in heat transfer occurs. We conducted the DSC testing (Power compensated DSC) of a PPXC film, resulting in the T_g of *ca* 52°C (Table 1). However, the T_g of PPXC from DSC is not that obvious in comparison to the other polymers. To address this issue, herein we systematically study parylene's viscoelasticity (primarily PPXC) with both Nano-DMA experiments [6] and MD simulations.

Few research studies were focused on the long term behavior of PPXC. The study of the PPXC's viscoelasticity can provide the answer to this issue. From the TTSP [7], the long-term parylene's viscoelastic properties can be predicted from short-term measurements. Since curves of the instantaneous modulus as a function of time do not change shape as the temperature is changed but only shift left or right. This implies TTSP can be adopted to predict the long-term performance of PPXC. By measuring PPXC's complex modulus at different temperatures and frequencies with Nano DMA testing mode, we can finally generate the master curve of PPXC for a specific temperature range.

SAMPLE PREPARATION

The preparation of PPXC samples is shown in Figure 1(a). A PPXC thin film of 1μm thickness was deposited on a planar substrate by SCS Labcoater (PDS 2010). The samples were then cut into several pieces of 10mm×10mm (Figure. 1 (b)). The SEM image (Figure. 1 (c)) shows the fabricated sample is of good quality. The tests were done by the Hysitron TI 950 Triboindentor (Figure 2(a)), using both quasi-static indentation and Nano DMA modes. Note that the as-deposited PPXC samples did not go through any processing step before testing.

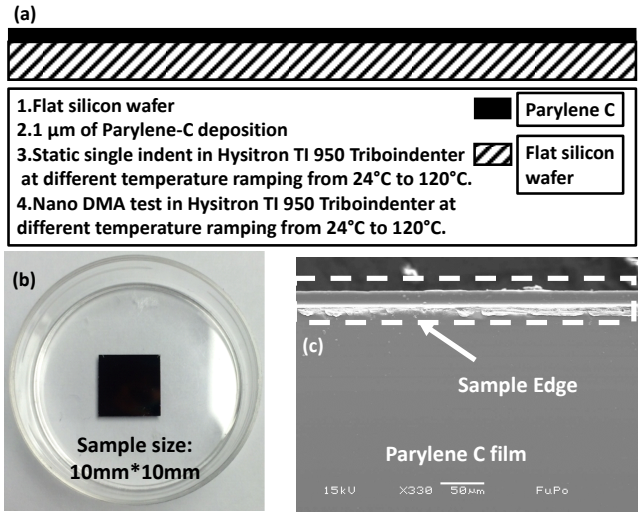

Figure 1: (a) Key fabrication steps of PPXC thin film samples; (b) The photograph of the fabricated sample; (c) SEM micrograph of a PPXC sample.

GLASS TRANSITION TEMPERATURE OF AS-DEPOSITED PPXC

Quasi-static Indentation

To measure the glass transition temperature (T_g) of our PPXC samples, a series of different temperature had been set in the quasi-static indentation tests. By placing the sample inside the environmental chamber (Figure 2(c)), the experimental temperature can be controlled and monitored. The tests were performed with samples at the temperatures ranging from 24°C to 120°C. The Berkovich tip with the three-sided pyramid was used in our test, which is a typical standard for nanoindentation. During the temperature ramping process, a series of quasi-static tests were performed with a static force of 50μN.

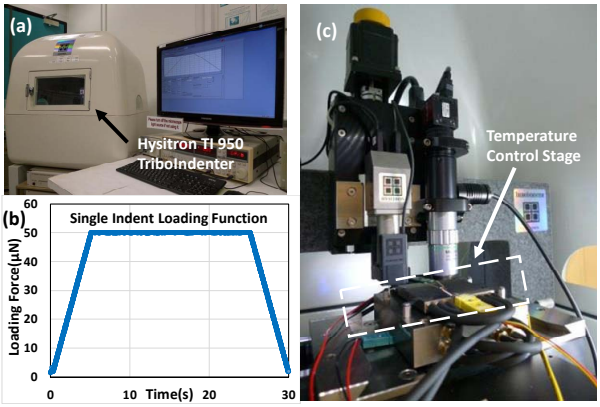

Figure 2: (a) Hysitron TI 950 Triboindenter; (b) Single indent loading function; (c) Temperature control stage.

Quasi-static testing comprises of four separate sections; the first section allows the machine to position itself at the surface of coating. The actual indenting process lasts 30s, the machine slowly increases the loading until the peak load is reached, and followed by 20s of maximum force and constant displacement to finish with the removal of the indenter tip for another 5s. The loading function of single indentation is shown in Figure 2(b).

The loading and unloading curves can be obtained from the quasi-static tests. With these data, PPXC's Young's modulus at different temperatures was calculated using the formula below:

$$h(t)^2 = \frac{\pi F}{2}\left(\frac{\pi}{3\sqrt{3}}\right)^{0.5}\frac{1}{(\tan\theta)^2}\frac{1}{E^*} \quad (1)$$

Here E^* is the Young's modulus described by Burgers model [7]:

$$\frac{1}{E^*} = \frac{1}{E_1^*} + \frac{1}{E_2^*}\left(1 - e^{-t\frac{E_2^*}{n_2}}\right) + \frac{t}{n_1} \quad (2)$$

where θ is the angle of the indenter tip which equals to 65.27° for Berkovich tip and h is the displacement in the indentation. Since we have performed the tests at different temperatures, we can observe the Young's modulus variation by graphing Young's modulus against temperature. From Figure 3, it can be observed that our results shows an sudden drop in the temperature range from 40°C to 50°C, which can be considered as the glass transition region of PPXC film samples. The result from quasi-static nanoindentation also shows good consistency with previous work (with TA Instruments Q800) [8], in which the T_g was determined as 50°C.

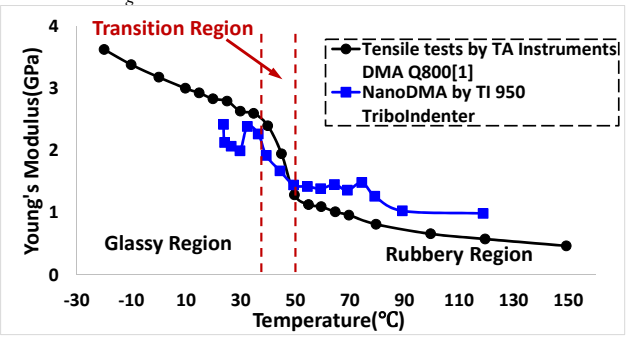

Figure 3: Young's modulus of PPXC as temperature varies.

MD Simulation

In order to avoid the effect of the thermal fluctuations around the periodic boundary layer [9], the total number of the initial PPXC structure is kept constant as 120,050 in simulation box, in which 25 molecular chains and 4802 atoms on each chain are included (Note that the volume density is close to a constant and does not increase anymore when the monomers on each chain is up to 300 for a given temperature from previous work [10]. Here n=300 monomers is built on each chain). The AMBER potential [11] is used among the present polymer chain. Each generated initial simulation box is annealed for 1 ns and controlled by the Nose-Hoover's thermostat until the pressure and energy of the system is stable, keeping both the given temperature T=600 K and the pressure P=1 atm (the time step dt=0.5 fs) in the NPT ensemble [12]. Afterward, the system is cooled down to be a given temperature in NPT ensemble and the density of the system is monitored, in which an effective cooling rate 1/20 (k/ps) should be controlled. The three directions of simulation boxes are subjected to the periodic boundary conditions. The LAMMPS software has been used to accomplish all MD simulations [13].

The MD simulation curves of the specific volume with the variation of temperature were shown in Figure 4. Each specific volume versus temperature curve for different polymers is fitted by two straight lines using the least squares method. The intersections of these two lines are marked as T_g.

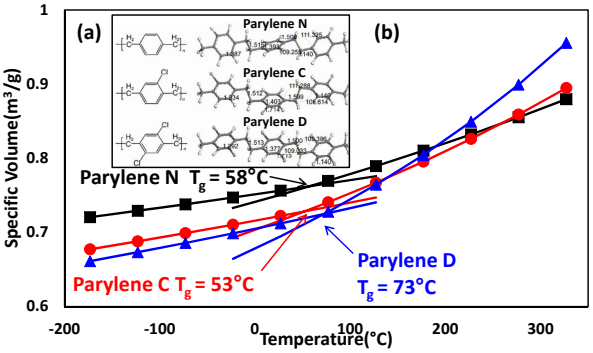

Figure 4: (a) Molecular formula of Parylene C/N/D; (b) MD simulation curves of the specific volume vs. temperature.

Table 1. Comparison of Glass Transition Temperature (T_g) of PPXC.

Samples	Methods	T_g(°C)
PPXC Film, ~3mg*	DSC	44[5]
PPXC Film, 21.5μm	Tensile Test	50[8]
PPXC-*120,050 atoms* *Simulation box:* *10.7×10.7×10.7 nm3* *(T=300 K)*	*Ab inito MD simulation,* *density*	53
PPXC Film, 1.55mg*	DSC	52
PPXC Film, 1μm	Nanoindentation	40-50

*Only the parylene sample weight can be reported in DSC.

PREDICT THE LONG TERM PERFORMANCE OF PPXC USING TTSP

Nano DMA technique with Hysitron TI 950 Triboindentor (Figure. 2(a)) was used to investigate the complex modulus (see Figure. 5(a)) for basic working principle) of PPXC thin films. According to TTSP, the long-term PPXC's viscoelastic properties can be predicted from short-term measurements.

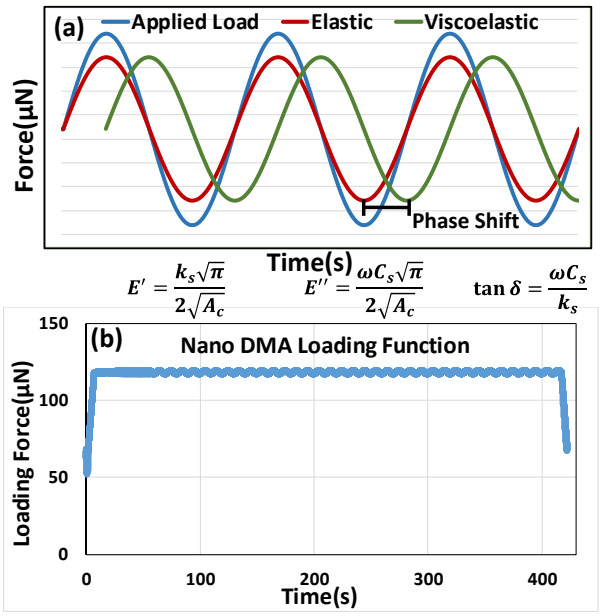

Figure 5: (a) Nano-DMA by applying sinusoidal loading force with different temperatures and frequencies; (b) Nano DMA loading function.

Creep test was conducted using Nano DMA testing mode. In Nano DMA tests, an initial indent was first made until the peak load is reached. Once the loading was stabilized, the indentation begins at maximal frequency and slowly decreases, all the indentation tests is done at peak force and standard settings. After the data collection process is over, the needle is removed from the sample. The dynamic loading function is shown in Figure 5(b).

Complex modulus under different temperatures can be obtained from Nano DMA tests. However, before we truly adopt TTSP into the experimental data analysis, what we need is to confirm that the deformation of PPXC film sample in the creep test is linear since the TTSP works under the principle of linear superposition. Other assumptions made are that the material does not undergo changes or phase transitions as a result of a change in temperature, the sample is homogeneous and the viscoelastic behavior is linear.

Since there is not enough theoretical methods to confirm the linear response of PPXC samples under different temperatures, we decided to plot the different storage modulus at 42 °C, which was below its T_g, 50°C. To confirm that testing could be done between 30 and 50μN, a temperature below the glass transition temperature, 50°C, was chosen. The results were positive as the slope at 50 and 30 μN are nearly identical. Since results for the storage modulus were nearly identical at both below and above T_g for peak loads of 30 to 50 μN, this confirms that the strain is linear. Having already proven that viscoelastic behavior of PPXC is linear, TTSP can be used below the melting point of PPXC.

Here the reference temperature is chosen as body temperature, 37°C, since the bionic devices on which PPXC is deposited will be working at a wide range of different frequencies in the body.

When trying to plot storage modulus at different frequencies and temperatures, it's found that the values at 60 and 70 °C had some intersections with data at other temperatures. A hypothesis to explain this peculiarity is that the material has just passed the glass transition temperature and may still be in the process of transiting from a hard structure to a softer substance. This may cause some parts of it to behave as a solid and other to behave as a rubber-like substance, which will probably lead an abnormal increase in storage modulus. After excluding the values at 60 and 70 °C, there is a trend showing that the values keep decreasing when temperature increases. The storage modulus at different frequencies and temperatures was plotted in Figure 6(a).

In TTSP, each curve is shifted by a shift factor, log(a), which can be calculated through either the Arrhenius equation:

$$a_{arrhenius} = \exp[\frac{E_a}{R} * (\frac{1}{T} - \frac{1}{T_0})] \quad (3)$$

or the Williams-Landel-Ferry (WLF) formula:

$$\log(a_{WLF}) = \frac{-C_1(T - T_0)}{C_2 + (T - T_0)} \quad (4)$$

where T is the temperature in Kelvin, T_0 is the reference temperature in Kelvin, E_a is the activation energy and R is the universal gas constant, C_1 and C_2 are empirical constants adjusted to fit the values of the shift factor. The WLF method is adopted since the Arrhenius experiments is solely used for chemical reactions.

To calculate C_1 and C_2, the shift factor was approximated for each curve to create the perfect master curve, from there the values of these constants were deduced. Since both the shift factor and the change in temperature is known, C_1 versus C_2 can be plotted to calculate these unknown values.

Rearranging the equation for the shift factor:

$$C_2(\log(a_{WLF})/(T - T_0)) + \log(a_{WLF}) = -C_1 \quad (5)$$

in the plot of C_1 versus C_2, there was a clear difference between the curves below and above 50°C, which confirmed that the T_g occurred in that region again. The values of C_1 and C_2 below 50°C and above it can be found by fitting all the data sets (Table 2).

Table 2. Empirical Constants for the master curve of PPXC at 37°C.

Constant	Above T_g	Below T_g
C_1	*31.5*	24
C_2	*1*	1.6

Once the values of C_1 and C_2 were found, the actual shift factor can be calculated for curves at different temperatures. In consequence, the master curve at 37°C

can be plotted in Figure 6(a)).

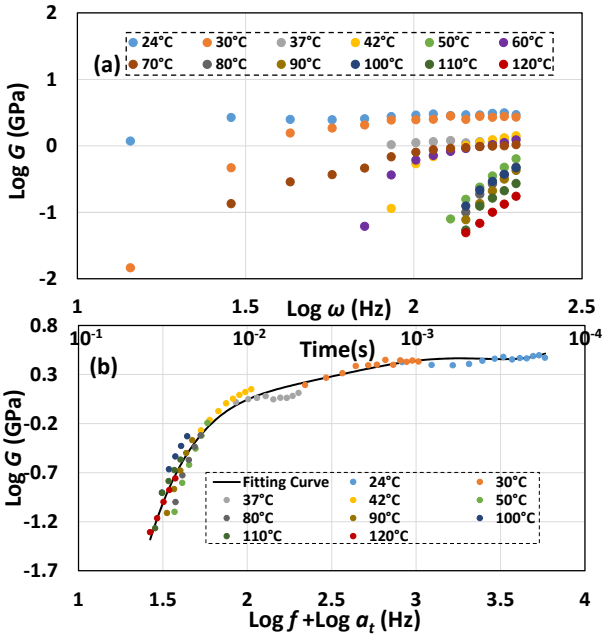

Figure 6. (a)Temperature dependence of elastic modulus of PPXC thin film at different frequencies; (b)The master curve for PPXC based on the nano-DMA experiments.

CONCLUSION

The PPXC's Young's modulus (with TI 950 Tribointenter) as a function of temperature, was consistent with that in the previous work (with TA Instruments Q800) (Figure 3) [8]. In addition, the T_g from Ref [8] was 50°C, while the measured curve in the present work (Figure. 2) showed the transition region around 40~50°C. The differential scanning calorimetry (DSC) also showed a T_g of *ca* 52°C. By examining the location of the transition of the specific volume as a function of temperature in the MD simulations (Figure. 4), T_g of PPXC can be identified as 53°C, consistent with these measured results. Thus MD simulation can be used to calculate the T_g of the other parylene materials, such as parylene N and parylene D, useful for the study of parylene samples difficult to be fabricated (Table 3). The elastic modulus as a function of driving frequency in Figure. 6 (a) highly depended on the operation temperature. With the master curve in Figure. 4(b), it is clearly that the parylene's elastic modulus dramatically decreased (i.e., degrade) when the temperatures were high (80°C ~120°C) at low frequency range.

Table 3. Comparison of Glass Transition Temperature (T_g) of Parylene C, N and D.

Samples	Methods	T_g (°C)
Parylene C	*MD simulation*	53
Parylene N	*MD simulation*	58
Parylene D	*MD simulation*	73

ACKNOWLEDGEMENTS

This work was sponsored by a research grant of HKUST (Ref No. FP007).

REFERENCES

[1] T. A. Harder, T. Yao, Q. He, et al., "Residual stress in thin-film parylene-c", in *IEEE MEMS 2017 Conference*, Las Vegas, Jan 24-24. 2002.

[2] C. Hassler, R. von Metzen, P. Ruther, et al., "Characterization of parylene C as an encapsulation material for implanted neural prostheses", *Journal of Biomedical Material Research,* vol. 93B, pp. 266-274, 2010.

[3] J. J. Senkevich, S. Desu, "Morphology of poly(chloro-p-xylylene) CVD thin films", *Polymer*, vol. 40, pp. 5751-5759, 1998.

[4] P. Tewari, R. Rajagopalan, E. Furman, "Control of interfaces on electrical properties of SiO2–Parylene-C laminar composite dielectrics", *Journal of Colloid Science*, vol. 332, pp. 65-73, 2009.

[5] S. Dabral, G. R. Yang, H. Bakhru, et al., "Chromium as an adhesion promoter/diffusion barrier for Cu on parylene", in *VLSI Multilevel Interconnection Conference*, New York, June 11-12, 1991.

[6] M Hull, D. Bowman, *Nanotechnology Environmental Health and Safety: Risks, Regulation and Management*, Elsevier, 2010.

[7] W. N. Findley, F. A. Davis, *Creep and Relaxation of Nonlinear Viscoelastic Materials*, Dover publication, 1989.

[8] J. C.-H. Lin, P. Deng, G. Lam, et al., "Creep of parylene-C film", in *IEEE Transduces 2011 Conference*, Beijing, China, June 5-9, 2011.

[9] F.M. Capaldi, M.C. Boyce, G.C. Rutledge, "Morphology of poly(chloro-p-xylylene) CVD thin films", *Polymer*, vol. 45, pp. 1391-1399, 2004.

[10] J. Zhao, L. Lu, T. Rabczuk, "Thermal conductivity of carbon nanocoils", *Comput. Mater. Sci.*, vol. 96, pp. 567-572, 2014.

[11] W.D. Cornell, P. Cieplak, C.I. Bayly, et al., "A second Generation force field for the simulation of poteins, nucleic acids, and organic molecules", *J. Am. Chem. Soc.*, vol. 117, pp. 5179-5197, 1995.

[12] S. Nose, "A unified formulation of the constant temperature molecular dynamics methods", *Phys.*, vol. 81, pp. 511-519, 1984.

[13] S. Plimpton, "Fast Parallel Algorithms for Short-Range Molecular Dynamics", *J. Comput. Phys.*, vol. 117, pp. 1-19, 1995.

CONTACT

*Y.-K. Lee, tel: +852-2358-8663; meyklee@ust.hk